Experimental observation of bulk and edge transport in photonic Lieb lattices

2014 New J. Phys. 16 063061

(http://iopscience.iop.org/1367-2630/16/6/063061)

New Journal of Physics
The open access journal at the forefront of physics
Deutsche Physikalische Gesellschaft DPG | IOP Institute of Physics

Experimental observation of bulk and edge transport in photonic Lieb lattices

D Guzmán-Silva[1,4], C Mejía-Cortés[1], M A Bandres[2], M C Rechtsman[2], S Weimann[3], S Nolte[3], M Segev[2], A Szameit[3] and R A Vicencio[1]

[1] Departamento de Física, MSI-Nucleus on Advanced Optics, and Center for Optics and Photonics (CEFOP), Facultad de Ciencias, Universidad de Chile, Santiago, Chile
[2] Physics Department and Solid State Institute, Technion, 32000 Haifa, Israel
[3] Institute of Applied Physics, Friedrich-Schiller-Universität Jena, Max-Wien-Platz 1, D-07743 Jena, Germany
E-mail: rodrigov@uchile.cl

Received 11 February 2014, revised 14 May 2014
Accepted for publication 27 May 2014
Published 26 June 2014

New Journal of Physics **16** (2014) 063061

doi:10.1088/1367-2630/16/6/063061

Abstract

We analyze the transport of light in the bulk and at the edge of photonic Lieb lattices, whose unique feature is the existence of a flat band representing stationary states in the middle of the band structure that can form localized bulk states. We find that transport in bulk Lieb lattices is significantly affected by the particular excitation site within the unit cell, due to overlap with the flat band states. Additionally, we demonstrate the existence of new edge states in anisotropic Lieb lattices. These states arise due to a virtual defect at the lattice edges and are not described by the standard tight-binding model.

Keywords: waveguide lattices, periodic structures, edge states

1. Introduction

A 'flat band' is a dispersionless energy band composed of entirely degenerate states. As a result of this degeneracy, any superposition of these states (even a highly localized one) is completely static, displaying no evolution dynamics whatsoever. Flat bands are manifested in a variety of

[4] Author to whom any correspondence should be addressed.

condensed matter contexts, including ferromagnetic ground states of Hubbard models [1], frustrated hopping models [2], in the context of localization in the presence of magnetic fields or spin–orbit coupling [3], and the fractional quantum Hall effect [4]. With the advent of the recent experimental observations of photonic topological insulators [5, 6], topological flat band models are now ripe for study in the optical domain. Indeed in optics, flat bands have direct technological relevance due to their high degeneracy, and thus high photonic density-of-states, leading to enhanced light-matter interaction [7]. Additionally, for Kagome–lattices single peak solitons have been shown to bifurcate from the flat band at zero power threshold [8], and a non-diffractive image transmission scheme has been suggested in the linear regime [9], showing the chance for concrete applications emerging from the flat band properties.

In the Lieb lattice—a line-centered square lattice—a flat band touches two linearly dispersing intersecting bands, i.e., the flat band intersects a single Dirac point. In the low-energy regime, the dispersion is described by a quasi-relativistic equation for spin-one fermions [10]. It is manifested in, e.g., the high-temperature tetragonal phases of the so-called cuprates: layered, ceramic materials that exhibit the phenomenon of high-temperature superconductivity [11]. In this particular system, several studies were conducted only recently, experimentally probing its response to external gauge fields [12] to nematic ferromagnetism [13] and nonlinear conical diffraction [14]. Flat bands exhibit various peculiar features [15–17] and, hence, deserve particular attention.

Here, we analyze transport in Lieb lattices theoretically and experimentally, in the bulk and at the edges. We demonstrate that whether or not flat-band modes are excited strongly impacts the transport in the bulk of the lattice. Additionally, we demonstrate the presence of Tamm-like edge states that arise at a van Hove singularity in the band structure [18]. Finally, we show that our photonic realization holds promise for a thorough analysis of various features of the Lieb lattice in terms of transport at and far from the lattice edges.

2. Bulk transport

The structure of the Lieb lattice is shown in figure 1(a), where it is evident that the unit cell consists of three sites, A, B and C. As in honeycomb lattices (also known as 'photonic graphene') [19], the equation describing the propagation of light in this system is

$$i\frac{\partial}{\partial z}\psi(x, y, z) = -\frac{1}{2k_0 n_0}\nabla_\perp^2\psi(x, y, z) - k_0\Delta n(x, y)\psi(x, y, z) \equiv H_{\text{cont}}\psi(x, y, z) \tag{1}$$

where z is the longitudinal propagation distance into the photonic lattice (playing the role of time in the analogous Schrödinger equation); ψ is the envelope of the electric field, defined by $E(x, y, z) = \psi(x, y, z)\,e^{i(k_0 z-\omega t)}$ (E is the electric field, k_0 the wavenumber in free space, $\omega = ck_0/n_0$ and c is the speed of light in vacuum); $\Delta n(x, y)$ is the refractive index structure defining the photonic lattice, n_0 is the refractive index of the material in which the lattice is embedded; $\nabla_\perp^2 = \partial_x^2 + \partial_y^2$ is the transverse Laplacian operator; H_{cont} as defined in equation (1) corresponds to the continuum Hamiltonian for wave propagation in a photonic lattice. Since the refractive index structure is composed of highly confined waveguides, each with a single bound state, we may employ a tight-binding approximation. Since within a given unit cell hopping takes place only between A–B and B–C nearest neighbors, the corresponding tight-binding Hamiltonian reads

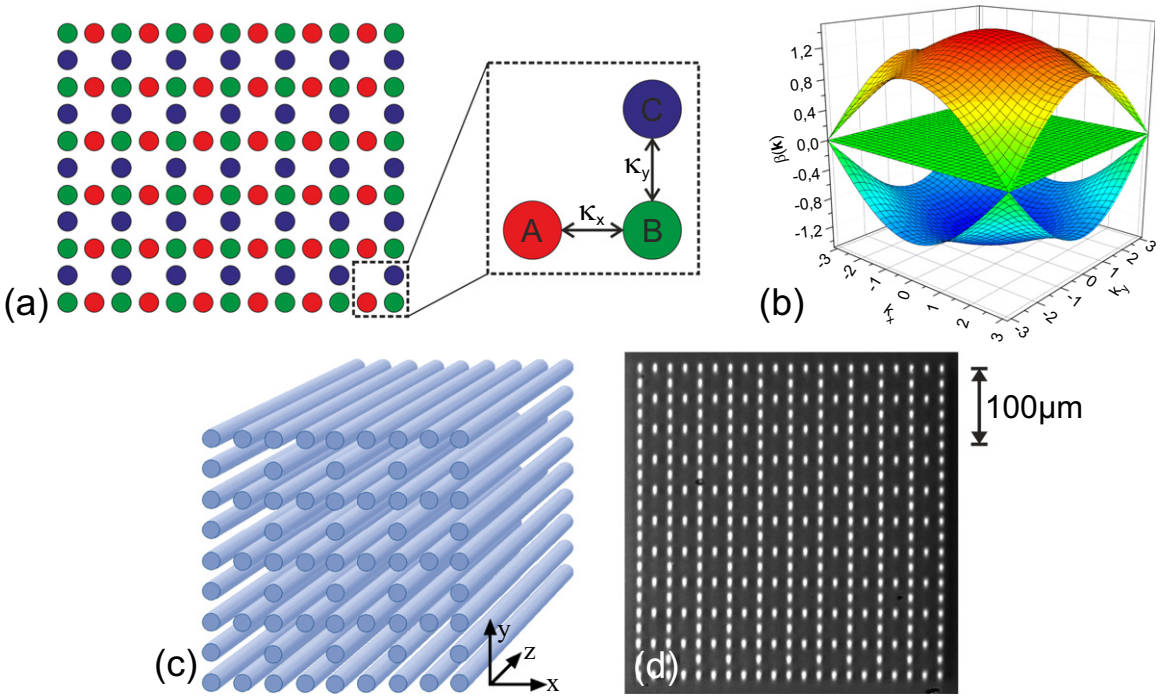

Figure 1. (a) Sketch of a Lieb lattice with three elements per unit cell. The hopping between A and B is described by κ_x (horizontal direction), and between B and C by κ_y (vertical direction). (b) The dispersion relation of the isotropic Lieb lattice ($\kappa_x = \kappa_y$) in the tight-binding approximation (equation (4)) shows three bands: a flat band at $\beta = 0$ and two conically intersecting ones, with all three bands intersecting at the M point ($k_x = k_y = \pi$). (c) Three-dimensional sketch of the waveguide arrangement. (d) Microscope image of white light output of a laser-written Lieb lattice in a fused silica glass wafer.

$$H_{\mathrm{TB}} = \sum_{n,m} \left[\kappa_x b_{nm}^{\dagger} \left(a_{nm} + a_{n+1,m} \right) + \kappa_y b_{nm}^{\dagger} \left(c_{nm} + c_{n,m-1} \right) + \mathrm{h.c.} \right], \tag{2}$$

where $a_{nm}^{\dagger}$, $b_{nm}^{\dagger}$, $c_{nm}^{\dagger}$ are the creation operators in the (n, m)th unit cell on the A, B and C sites, respectively. The summation takes place over $n, m \in \mathbb{R}$ and $\kappa_{x,y}$ are the inter-site couplings in the x- and y-direction. Now, transforming to momentum space by defining $\Psi_{\mathbf{k}}^{\dagger} = \left(\mathrm{e}^{ik_x/2} a_{\mathbf{k}}^{\dagger}, b_{\mathbf{k}}^{\dagger}. \mathrm{e}^{-ik_y/2} c_{\mathbf{k}}^{\dagger} \right)$, where $a_{\mathbf{k}} = (2\pi)^{-1} \sum_{nm} a_{nm} \exp\left(ik_x n + ik_y m \right)$, (and similarly for all the other operators), the real-space Hamiltonian becomes in Fourier space, $H_{\mathrm{TB}} = \int \Psi_{\mathbf{k}}^{\dagger} \mathcal{H}_{\mathrm{TB}} \Psi_{\mathbf{k}} \mathrm{d}k$, where

$$\mathcal{H}_{\mathrm{TB}} = 2 \begin{pmatrix} 0 & \kappa_x \cos\left(k_x/2\right) & 0 \\ \kappa_x \cos\left(k_x/2\right) & 0 & \kappa_y \cos\left(k_y/2\right) \\ 0 & \kappa_y \cos\left(k_y/2\right) & 0 \end{pmatrix} \tag{3}$$

with $k_{x,y} \in [-\pi, \pi]$ (first Brillouin zone). From this, one readily obtains the dispersion relation, i.e., the spectrum

$$\beta(\mathbf{k}) = 0;\ \pm 2\sqrt{\kappa_x^2 \cos^2\left(k_x/2\right) + \kappa_y^2 \cos^2\left(k_y/2\right)}. \tag{4}$$

The full spectrum (shown in figure 1(b) for $\kappa_x = \kappa_y = 1$) consists of three bands: a flat band ($\beta(\mathbf{k}) = 0$) and two conically intersecting bands, with all three bands intersecting at the M point ($k_x = k_y = \pi$). Note that for each eigenstate at Bloch wavevector $\mathbf{k}$ in the top band with eigenvalue β, there exists an eigenstate also at $\mathbf{k}$ with eigenvalue $-\beta$; this is known as particle–hole symmetry [20]. The eigenfunctions of the finite Lieb lattice with periodic and vanishing boundary conditions are given in [15]. Importantly, any superposition of eigenstates belonging to the flat band is also an eigenstate of the system, meaning that it is static and does not contribute to transport. Equivalently, the group velocity in the flat band is zero at all Bloch wave vectors, therefore any wavepacket is necessarily diffraction-free. Consequently, to have transport, states in the other bands have to be excited. We also note that the flat band is not destroyed by any anisotropy (i.e., $\kappa_x \neq \kappa_y$), being an intrinsic property of this lattice in the nearest-neighbor coupling limit [14].

In general, linear modes of any periodic structure are completely extended. However, flat band systems allow the formation of very localized eigenmodes as a destructive linear combination of extended linear wavefunctions [22]. In the case of the Lieb lattice, in any square of the lattice (formed by four B sites at the corners, two C sites at the upper and lower sides and two A sites at the right and left sides of the square) a stationary localized mode can be created by taking the four B sites strictly zero, the two C sites with an amplitude ψ_C, the last two A sites with an amplitude $\psi_A = -\kappa_y \psi_C/\kappa_x$ and the rest of lattice sites zero.

For our experiments, we fabricate Lieb lattices employing the laser direct-write technology [21]. To this end, ultrashort laser pulses (Coherent Mira/RegA, $\lambda = 800$ nm, $t_p \approx 200$ fs at 100 kHz repetition rate) are tightly focused through a microscope objective (25×, NA = 0.35) into a 10 cm long transparent fused silica wafer and translated by means of a high-precision positioning system (Aerotech). In that way, we create a three-dimensional structure with a Lieb lattice in the transverse plane that is preserved along the propagation axis. A microscope output view of such a lattice, which consists of 341 waveguides with nearest-neighbor spacing of 20 μm, is shown in figure 1(c) (for this image we propagate white light and take an image at the output facet, where white corresponds to the light propagating in each waveguide and gray to the bulk silica). Note that due to the slightly elliptical form of our waveguides, we find that the vertical inter-site coupling is slightly stronger than the horizontal one, i.e. the lattice is effectively uniaxially strained and anisotropic with $\kappa_y \approx 1.5\kappa_x$. In our experiments, laser light at $\lambda = 637$ nm was launched into a single waveguide at the input facet of the array using a standard microscope objective. At the output facet of the sample, intensity patterns were recorded with a CCD camera.

We begin by launching light into the bulk of the lattice, i.e., far away from the edges. As there are three elements per unit cell (see figure 1(a)), we study the propagation arising from excitations in each of the three positions A, B and C. The corresponding diffraction patterns obtained in our experiments are shown in figures 2(a), (b), (c). One can clearly see that the impact of the excitation location on the diffraction pattern is significant, depending on where in the unit cell the lattice is excited. The reason lies in the unique structure of the Lieb lattice, where a single site excitation (that corresponds to a unit impulse in real space) does not necessarily excite all bands—in contrast with some other lattices with multipartite unit cells,

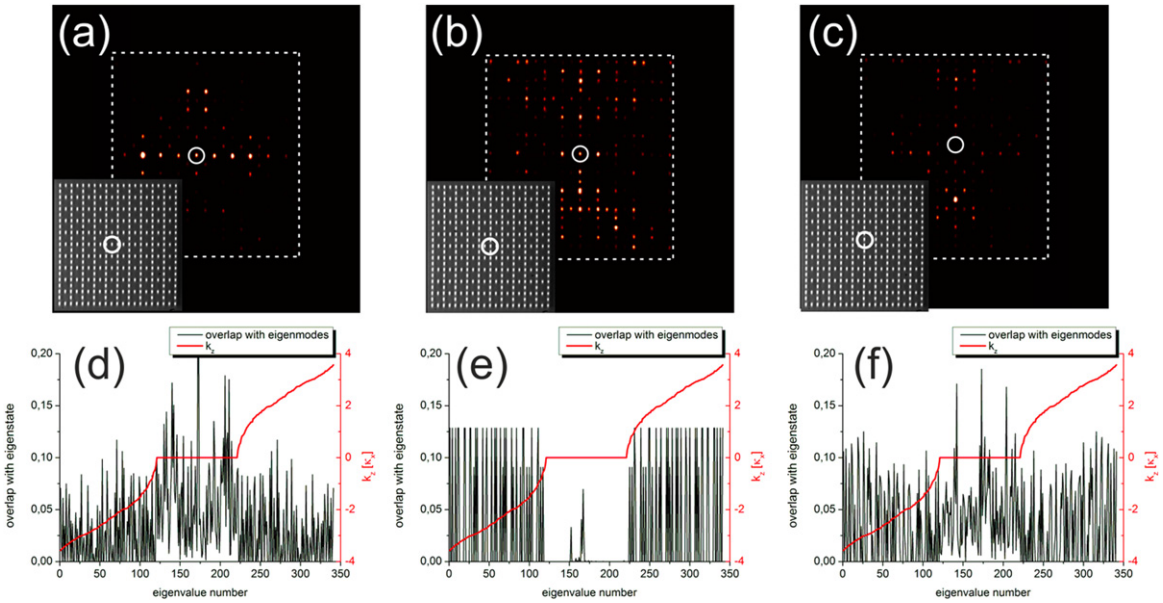

Figure 2. Experimentally observed light distribution at the output facet of the lattice, when exciting (a) the *A*-site, (b) the *B*-site and (c) the *C*-site. The overlap with the eigenmodes in the three bands is shown in (d) for the *A*-site, (e) for the *B*-site and (f) for the *C*-site. It is evident that transport is stronger when the flat band is least populated at the initial plane of excitation.

such as the honeycomb lattice. To illustrate this effect, we plot the projections $P = \langle k, j|\psi^{\text{excit}}\rangle$ of the impulse excitation $|\psi^{\text{excit}}\rangle$ at the *A*, *B*, or *C* sites on the eigenfunctions $|k, j\rangle$ of the three bands (j is the band index) in figures 2(d), (e), (f), and compare them to the experimental data. It is evident that, when exciting the *B* site (figure 2(e)), the projections on the flat band are minimal (equal to $1/(N+1)^2$, where N is the number of complete unit cells on one side of a finite square Lieb lattice, i.e., $N = 10$ in our case) and, hence, transport is strong. This is clearly observed in the experiment (see 2(b)), where the light spreads across many lattice sites following the 10 cm propagation in the lattice. However, when exciting the *A* site the situation changes drastically (figure 2(d)). In this case, the projections on the flat band dominate and, therefore, the transport is minimal. The experiment shows exactly this: the spreading is very weak, and the light covers only a few lattice sites after propagating through the lattice (see figure 2(a)). Intermediate spreading is observed when launching light into lattice site *C*, as shown in figure 2(c), as a consequence of the partial overlap with the flat band (see figure 2(f)).

At this point it is interesting to examine the transport through the Lieb lattice when strain is applied. Specifically, it has been shown that inhomogeneous strain applied to honeycomb lattices can give rise to Landau level splitting [23], robust Klein tunneling [24], topological transitions [25], and other unexpected phenomena. It is therefore instructive to look at the projections on the flat band as a function of the strain when exciting either the *A*, *B* or *C* sites in the infinite Lieb lattice. Our calculations are summarized in figure 3. Interestingly, when exciting a *B* site, the population of the flat band always vanishes, for all values of the anisotropy. Localized flat band modes have *B* sites with zero amplitude, therefore launching light into this site will always result in strong transport, irrespective of the ratio κ_y/κ_x. However,

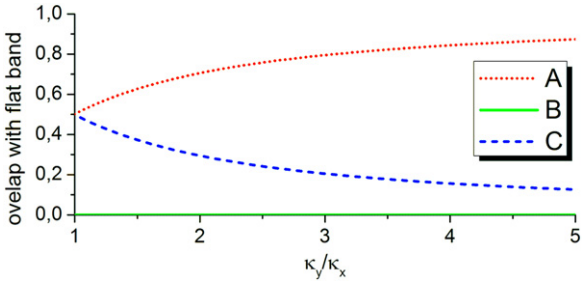

Figure 3. The overlap of single-site excitation with flat band modes, for excitation of the *A*-site (red dotted line), *B*-site (green solid line) and *C*-site (blue dashed line).

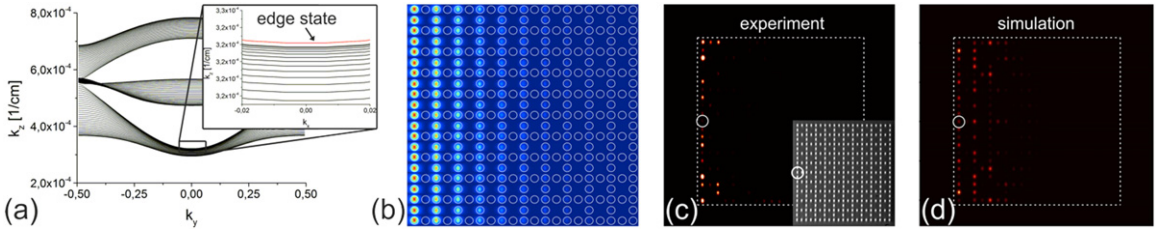

Figure 4. (a) Edge band structure of a strained Lieb lattice ($\kappa_y = 1.5\kappa_x$) using the continuous model equation (1), showing the appearance of edge states (red line). (b) The intensity distribution of the edge state in the Lieb lattice. (c) Experimental observation of the edge states after an impulse excitation. (d) Simulation of the light diffraction at the edge.

the situation is different for an excitation of the *A* and *C* sites. Whereas for the isotropic case ($\kappa_x = \kappa_y$), the overlap with the flat band for both sites is exactly the same (due to symmetry), for the anisotropic case ($\kappa_y > \kappa_x$) the flat band is more populated for an *A*-site excitation (resulting in decreasing transport) and less populated for a *C*-site excitation (yielding enhanced transport). Anisotropic $\beta = 0$ modes have $|\psi_A| > |\psi_C|$, therefore the overlap is stronger with A-site excitation.

3. Edge transport

Besides the bulk transport, we pay particular attention to the diffraction of light at the edge of the lattice. As we described above, the flat band can form localized modes. It is important to note that these flat band localized modes can be located at the edge of the lattice. However, we find surprisingly that edge states that do not lie on the flat band arise in anisotropic Lieb lattices in the continuous model (equation (1)). In figure 4(a) we present a plot of the band structure at the edge of the Lieb lattice by diagonalizing H_{cont} as given by equation (1), showing clearly the existence of states emerging from the bulk bands that are localized at the lattice edge. The underlying mechanism for the formation of these edge states is similar to the one recently reported for 'photonic graphene' [18]. Note that these calculations are performed by fully diagonalizing H_{cont}, as given in equation (1), as opposed to simply examining the spectrum of the tight-binding model.

To explain these edge states in the Lieb lattice, one has to take into account the fact that the effective on-site propagation constant of each mode is modified by its neighboring sites. This modification differentiates between the *B*-sites in the bulk, where they have four neighbors, and the edge, where they have only three. Although this difference is small and is usually neglected in tight-binding theories, it comes into play where the modes are highly degenerate at the van Hove singularity. At the degeneracy point, a slight edge perturbation can take the edge mode out of the band and create a Tamm-like edge state as shown in figure 4(b). We emphasize again that this state does not result from any real surface perturbation but rather from the specific surface structure along the edge. We classify this state as a 'Tamm state' [25] as opposed to a 'Shockley state' [27], because it does not arise due to a band crossing, the criterion for the emergence of Shockley states. It is important to note that these states do not have a topological origin, and only arise from the 'effective defect' at the edge. Therefore, they must come in counterpropagating pairs; and any defect on the edge will allow scattering between these. Although Tamm states are conventionally associated with surface perturbations or defects (that are inherent in the system, or that arise from modulation [28]), in the present case no defects whatsoever are present. Instead, what happens here is that the edge itself acts as a sufficiently strong defect to localize light on the edge. This effect cannot be accounted for in the standard tight-binding model and appears only in the continuum model. The experimental observation of strong edge diffraction in the anisotropic Lieb lattice is presented in figure 4(c), the simulations using equation (1) are shown in figure 4(d). It is important to note that we are exciting B sites at the edge and that as we described above, B-site excitations do not couple to flat band modes. Therefore, by exciting a site 'B', we know that the observed edge state does not belong to the flat band and that it is indeed exciting the new state that we found in the continuous model. This stands in contrast to the top and bottom edges, where there are no edge states at all in the continuum model. The breaking of symmetry between the top/bottom termination and the left/right termination stems from the anisotropy of the waveguides. As a result, when light is injected into waveguides on the top or bottom of the structure, strong bulk diffraction (and little edge confinement) is observed. This signifies that there is no edge state of the continuous model on the top and bottom edges, as has been observed in the left and right edges.

4. Conclusions

In conclusion, we presented a theoretical and experimental study of transport of light in photonic Lieb lattices. We find that the transport in the bulk is significantly affected by which site in the unit cell is excited, due to different overlap with the flat band (since any superposition of flat band states does not diffract and can form localized bulk states). Importantly, an excitation of the *B*-site in the unit cell leaves the flat band essentially empty, resulting in maximal transport. We also show that the population of the different bands is a function of the anisotropy of the lattice. Moreover, we demonstrate the existence of new edge states in anisotropic Lieb lattices that arise due to a virtual defect at the lattice edges and are not manifested in the standard tight-binding model. Our findings experimentally prove that the Lieb lattice exhibits various peculiar and unique features concerning wave transport, which might find their way into new concepts for imaging, routing and switching.

Acknowledgments

The authors wish to thank the German Ministry of Education and Research (Center for Innovation Competence programme, grant 03Z1HN31), and the Thuringian Ministry for Education, Science and Culture (Research group Spacetime, grant 11027-514), FONDECYT Grants 1110142 and 3140608, Programa ICM P10-030-F, Programa de Financiamiento Basal de CONICYT (FB0824/2008), and the Consejo Nacional de Ciencia y Tecnología, México.

References

[1] Tasaki H 2008 *Eur. Phys. J.* B **64** 365
[2] Bergman D L, Wu C and Balents L 2008 *Phys. Rev.* B **78** 125104
[3] Vidal J, Mosseri R and Doucot B 1998 *Phys. Rev. Lett.* **81** 5888
[4] Neupert T, Santos L, Chamon C and Mudry C 2011 *Phys. Rev. Lett.* **106** 236804
[5] Rechtsman M C, Zeuner J M, Plotnik Y, Lumer Y, Podolsky D, Dreisow F, Nolte S, Segev M and Szameit A 2013 *Nature* **496** 196
[6] Hafezi M, Mittal S, Fan J, Migdall A and Taylor J 2013 *Nat. Photonics* **7** 1001
[7] Wang Z, Chong Y, Joannopoulos J D and Soljacic M 2009 *Nature* **461** 772
[8] Vicencio R A and Johansson M 2013 *Phys. Rev.* A **87** 061803(R)
[9] Vicencio R A and Mejía-Cortés C 2014 *J. Opt.* **16** 015706
[10] Shen R, Shao L B, Wang B and Xing D Y 2010 *Phys. Rev.* B **81** 041410(R)
[11] Bednorz J G and Müller K A 1986 *Z. Phys.* B **64** 189
[12] Goldman N, Urban D F and Bercioux D 2011 *Phys. Rev.* A **83** 063601
[13] Zhang W 2012 arXiv:1201.0722
[14] Leykam D, Bahat-Treidel O and Desyatnikov A S 2012 *Phys. Rev.* A **86** 031805(R)
[15] Nita M, Ostahie B and Aldea A 2013 *Phys. Rev.* B **87** 125428
[16] Leykam D, Flach D, Bahat-Treidel O and Desyatnikov A S 2013 *Phys. Rev.* B **88** 224203
[17] Flach S, Leykam D, Bodyfelt J D, Matthies P and Desyatnikov A S 2014 *Eur. Phys. Lett.* **105** 30001
[18] Plotnik Y *et al* 2014 *Nat. Mater.* **13** 5762
[19] Peleg O, Bartal G, Freedman B, Manela O, Segev M and Christodoulides D N 2007 *Phys. Rev. Lett.* **98** 103901
[20] He J, Zhu Y-X, Wu Y-J, Liu L-F, Liang Y and Kou S-P 2013 *Phys. Rev.* B **87** 075126
[21] Bergman D L, Wu C and Balents L 2008 *Phys. Rev.* B **78** 125104
[22] Szameit A and Nolte S 2010 *J. Phys. B: At. Mol. Opt. Phys.* **43** 163001
[23] Rechtsman M C, Zeuner J M, Heinrich M, Tunnermann A, Segev M and Szameit A 2013 *Nat. Photonics* **7** 153
[24] Bahat-Treidel O, Peleg O, Grobman M, Shapira N, Segev M and Pereg-Barnea T 2010 *Phys. Rev. Lett.* **104** 063901
[25] Rechtsman M C, Plotnik Y, Zeuner J M, Song D, Chen Z, Szameit A and Segev M 2013 *Phys. Rev. Lett.* **111** 103901
[26] Tamm I 1932 *Z. Phys.* **76** 849
[27] Shockley W 1939 *Phys. Rev.* **56** 317
[28] Szameit A, Garanovich I L, Heinrich M, Sukhorukov A A, Dreisow F, Pertsch T, Nolte S, Tünnermann A and Kivshar Y S 2008 *Phys. Rev. Lett.* **101** 203902